

Electrografted anthraquinone to monitor pH at the biofilm-anode interface in a wastewater microbial fuel cell

Nazua L Costa, Germaine Olorounto, Estelle Lebègue, F Barriere

▶ **To cite this version:**

Nazua L Costa, Germaine Olorounto, Estelle Lebègue, F Barriere. Electrografted anthraquinone to monitor pH at the biofilm-anode interface in a wastewater microbial fuel cell. Colloids and Surfaces B: Biointerfaces, 2022, 210, pp.112274. 10.1016/j.colsurfb.2021.112274 . hal-03558756

HAL Id: hal-03558756
https://hal.science/hal-03558756

Submitted on 4 Feb 2022

HAL is a multi-disciplinary open access archive for the deposit and dissemination of scientific research documents, whether they are published or not. The documents may come from teaching and research institutions in France or abroad, or from public or private research centers.

L'archive ouverte pluridisciplinaire **HAL**, est destinée au dépôt et à la diffusion de documents scientifiques de niveau recherche, publiés ou non, émanant des établissements d'enseignement et de recherche français ou étrangers, des laboratoires publics ou privés.

Electrografted anthraquinone to monitor pH at the biofilm-anode interface in a wastewater microbial fuel cell

Summary of the total number of words and tables/figures in the manuscript

Number of Figures in article	**6**
Number of Table in article	**1**
Sum of "Figure" in article	**7**
Number of Figures in SI	**5**
Number of Table in SI	**0**
Sum of "Figure" in SI	**5**
Number of words in article (no references)	**4355**
Number of words in references	**702**
Number of words in Abstract	**147**
Number of words in Highlights	**59**
Number of Keywords	**6**

Electrografted anthraquinone to monitor pH at the biofilm-anode interface in a wastewater microbial fuel cell

Nazua L. Costa[†,¥]*, Germaine Olorounto[†], Estelle Lebègue[♠] and Frédéric Barrière[†]*

[†] Univ Rennes, CNRS, Institut des Sciences Chimiques de Rennes - UMR 6226, F-35000 Rennes, France.

[♠] Université de Nantes, CNRS, CEISAM UMR 6230, F-44000 Nantes, France.

[¥] Instituto de Tecnologia Química e Biológica António Xavier, Universidade NOVA de Lisboa, Av. da República-EAN, 2780-157, Oeiras, Portugal

***corresponding authors:** nazuacosta@itqb.unl.pt and frederic.barriere@univ-rennes1.fr

Keywords: aryldiazonium; surface modification; interfacial pH sensors; 1-aminoanthraquinone; cyclic voltammetry, electricigen bacteria

Abstract

Electrografted anthraquinone on graphite was used as a probe to monitor the pH change at the biofilm-electrode interface at the anode of a microbial fuel cell inoculated with wastewater. The grafting procedure was optimized so that the pH-dependent electrochemical response of the grafted quinone did not overlay with that of the electroactive biofilm. The variation of the formal potential of the grafted quinone as a function of pH was linear over the pH range 1 to 10 with a slope of -64 mV. This allowed to monitor the interfacial pH change over three weeks of biofilm colonization of the electrode. During that time the interfacial pH decreased from neutrality to 5.3 while the anolyte only acidified down to pH 6.2. This finding is relevant as local pH change usually leads to alterations of the bioenergetics process of microbial communities and hence on the performance of bioelectrochemical devices.

1. Introduction

Microorganisms that catalyze reactions in bioelectrochemical systems (BES) are known for their ability to exchange electrons with electrodes through a metabolic process called extracellular electron transfer. They are often found in well-organized symbiotic or commensal mixed biofilms and are qualified as electroactive [1,2]. On the surface of anodes, electroactive biofilms couple the oxidation of carbon sources like acetate or glucose with proton-releasing metabolic reactions via a network of redox active proteins that extends from the inner membrane towards the cell surface [3]. Whether extracellular electron transfer is made directly by surface-exposed membrane proteins contact with the solid or indirectly via redox shuttles [4], electron transfer is often coupled or associated to extracellular proton release to maintain cell electroneutrality and/or internal pH [5]. This in turn acidifies both the biofilm and the anolyte which may impact the bacteria metabolism. In Microbial Fuel Cells (MFCs), one of the most explored BES, electrons resulting from the oxidation of the organic matter by electroactive bacteria are accepted by the anode while the protons migrate through a proton exchange membrane towards the cathode [6]. However, around neutral pH and in concentrated buffer solutions, other cationic species are also responsible for the ionic current through the membrane [7] which can lead to proton accumulation in both the biofilm exopolysaccharide matrix and at the electrode-biofilm interface, and eventually in the anolyte of batch type systems. This acidification can impair microbial growth and current production in MFCs [8]. Although the effect of the electrolyte pH on the performance of anodic electroactive biofilms is well-known [9–12], few studies have yet reported how the pH evolves at the biofilm-electrode interface during turnover and non-turnover processes [13]. Methods for measuring pH at interfaces include electrochemical pH sensors, electrochemical scanning probe techniques, fluorescence and voltammetry. Localized and dynamic pH alteration and monitoring at biological nano-objects (enzymes) is possible with the coupling of scanning electrochemical microscopy with single-molecule fluorescence spectroscopy [14]. This additionally requires a confocal laser microscope or an internal reflection for fluorescence recording [14]. The scanning electrochemical microscopy technique using a 25 μm diameter platinum/iridium oxide pH-dependent ultramicroelectrode was also applied to the local pH change monitoring at the liquid-liquid water/organic interface induced by the photo-activated transfer of a photoactive compound [15]. A voltammetric pH nanosensor with high spatial resolution (5 μm) was designed by adsorbing a redox-active pH probe (in the

range pH 2-12) inside a carbon coated quartz nanopipette [16]. The pH gradient and alkalinization around a 10 μm diameter Pt disc electrode polarized for the reduction of oxygen was demonstrated in aerated phosphate buffer saline electrolyte (bulk pH 7.4) [16]. These examples of pH monitoring at interfaces with scanning electrochemical microscopy show the potential high resolution of the approach. Practical and technical limitations however are the equipment needed for the measurements and monitoring, and the scanning time needed for large samples or the scanning rate inadequate for fast and dynamic pH changes. Biofilms can cover large surface and may be several hundreds of micrometers thick or more so that mapping of pH in the three directions with fluorophores [10–12] and discrimination between intracellular and extracellular pH is important [12]. Integration of nanoparticles in biofilms [17] has been applied to the pH mapping within biofilms [18]. Mesoporous silica nanoparticles (ca. 47 nm diameter) functionalized with pH-dependent and independent dyes allowed the ratiometric fluorescence measurement of the pH distribution within biofilms of *Pseudomonas fluorescens* microcolonies [18]. The quantification of pH variations in electroactive biofilms is interesting for both fundamental and applied research that aims at improving the performance of BES as alternative energy harvesting resource. Herein we report the simple and straightforward voltametric measurement of the pH at the biofilm-electrode interface using electrodes modified with a pH-dependent redox-active probe.

To date anthraquinone (AQ)-based electrodes have been used as pH and oxygen sensing probes for chemical processes [19], to measure peroxide electrocatalysis [20], and more recently as grafted redox mediators for MFCs studies that aims at measuring the electron transfer rate from NAD^+/NADH to the electrode [21]. However, to our knowledge no study has yet reported these AQ-modified electrodes as biofilm-electrode interfacial pH probes. In the present study, 1-aminoanthraquinone (1-AAQ) was used to modify electrodes that were subsequently used as anodes in MFCs inoculated with wastewater in order to investigate the pH changes at the biofilm-electrode interface.

2. Experimental section

2.1 Chemicals and solutions

All solutions were prepared with Milli-Q water (18.2 MΩ cm). 1-Aminoanthraquinone was purchased from Alfa Aesar. Potassium dihydrogen phosphate, potassium hydrogen phosphate, sodium nitrite, potassium hexacyanoferrate (III) and glucose were obtained from Sigma Aldrich. Concentrated hydrochloric acid (2 M, 37%, ACS Reagent) and sodium hydroxide

pellets (ACS) were purchased from VWR. Commercial pH buffers were purchased from VWR BDH Chemicals (ACS TITRINORM grade) for pH 1 (glycine buffer, certified +/- 0.02 pH-units) and pH 2, 3, 5, 6, 8, 9, 10 (certified at +/- 0.05 pH-units) and from Merck Millipore for pH 4.01 (potassium hydrogen phthalate and pH 7.00 (potassium dihydrogen phosphate/disodium hydrogen phosphate), both of Certipur® grade. Buffers were all used at 0.1 M concentration.

2.2 Instrumentation and electrochemical measurements

Electrochemical experiments were performed at room temperature (19 ± 2°C) in a three-electrode set-up using an Autolab PGSTAT204 potentiostat/galvanostat (Eco Chemie B.V., the Netherlands) and Nova 2.14 as the electrochemical software (Metrohm). All potentials were reported versus an Ag/AgCl (3 M KCl) reference electrode with an estimated ± 1 mV uncertainty. A graphite rod was used as the counter electrode. The anodic chamber was degassed with argon bubbling and all measurements made under a constant argon flow above the anolyte.

2.3 Electrochemical analysis

The surface concentration (Γ) of AQ was calculated using $\Gamma = Q/nFA$ (mol/cm^2), where Q (C) = i (A) × t (s) the charge corresponding to the integration of the faradaic current produced by the redox active molecule, n = 2 the number of electrons involved in the electron transfer reaction, F the Faraday's constant and A the electrode surface area (cm^2). The evolution of the formal potential ($E^{0'}$) of the grafted anthraquinone / anthrahydroquinone redox couple with the pH of the electrolyte was determined by cyclic voltammetry (CV) for pH values ranging from 1 to 10. The calibration curve was drawn using the mean of 3 sets of independent experiments. Biofilm-electrode interfacial pH measurements were made using the calibration curve.

2.4 Surface modification

Graphite rods (Morgan Carbon, France) were isolated with Teflon tape to obtain controlled 5 mm diameter disk electrodes. The electrodes were polished with grit 500 SiC papers (Struers), prior to surface modification or direct incubation in MFCs as a negative control. All electrochemical experiments were performed in an anoxic environment by continuous argon purging. The 1-aminoanthraquinone grafting on graphite surfaces was performed in acidic aqueous solution (0.5 M) containing 1 mM of 1-aminoanthraquinone (1-AAQ) and 3 mM of

$NaNO_2$ incubated for 30 min before recording 10 cyclic voltamogramms (CVs) from +0.7 V to 0.0 V *vs.* Ag/AgCl (3 M KCl) at a scan rate of 50 mV/s. The AQ modified graphite electrode was then sonicated for 3 minutes in 0.1 M potassium phosphate buffer at pH 7 to remove unreacted salts and studied by CV in commercial buffer solutions at different pH values (1-10).

2.5 Microbial fuel cell operation and biofilm growth

An H type reactor was assembled as described previously [22,23]. A sketch of the reactor is provided as Figure S1. The initial inoculum was prepared using 100 mL of municipal wastewater (Beaurade Wastewater Treatment Plant, Rennes, France) and 200 mL of 100 mM potassium phosphate buffer at pH 7 for a total volume of 300 mL. 20 mM of glucose was added as selective carbon source. After one-hour argon purging, the pH of the inoculum was measured and adjusted to 7 using small amounts of concentrated HCl or NaOH aqueous solutions. Weekly pH measurements and adjustments to 7 were performed when needed. To maintain the anaerobic conditions the anodes were sealed using anaerobic rubber caps and argon purges were performed every two days. Aluminum foil was used to protect the chamber from sunlight thus avoiding the growth of phototrophic species. Aerobic cathode chamber was filled with 300 mL of 100 mM potassium phosphate buffer aqueous solution with 20 mM potassium hexacyanoferrate III to ensure a stable potential and a non-limiting cathodic current. The two MFC compartments were separated by a cation exchange membrane (Fumasep® FKS-PET-75, Fumatech, Germany). Both anodic and cathodic electrodes were connected by a 1.2 kΩ external resistance and kept in a 30°C thermostatic bath. A digital multimeter (Velleman DVM9912) was used to measure the potential difference between the electrodes. To monitor the biofilm formation, weekly CV at 10 mV/s was performed. After 1 month in operation, the inoculum of MFCs was replaced by 100 mM potassium phosphate buffer at pH 7.

3. Results and discussion

3.1 Electrochemical modification of the graphite surface by cathodic reduction of diazonium salt generated in-situ from 1-AAQ

Prior to the electrochemical modification, the acidic solution containing 1-AAQ (Fig. 1A) was put under stirring at 50°C for 30 minutes and was then left to further incubate for 40 minutes at room temperature after the addition of $NaNO_2$ to ensure the formation of the diazonium

cation. The reduction of the diazonium cation towards the formation of the radical is illustrated on Fig. 1B, where the first scan shows its characteristic irreversible reduction peak around +0.3 V *vs*. Ag/AgCl (3 M KCl) followed by the relative passivation of the electrode from the second scan onwards. The passivation results from a partial blocking of the interfacial electron transfer induced by the grafted AQ moieties onto the electrode surface [24,25]. After 10 recurrent CVs the electrode is passivated confirming the grafting of AQ moieties on the surface of the graphite electrode and thus the electrode surface modification [26]. The electrodes modified by this procedure will be hereafter referred to as 10-AQ.

Before evaluation of the 10-AQ-modified electrode a standard 3-minute sonication step, in 0.1 M potassium phosphate buffer, was performed to remove the non-grafted (adsorbed) species from the electrode surface. CV curves of bare graphite electrode and modified 10-AQ electrode were recorded at 50 mV/s in 0.1 M potassium buffer at pH 7 (Fig. 1C). While the CV of bare graphite (black) is featureless the 10-AQ electrode is characterized by two well defined chemically reversible redox couples at -0.55 V (peak 1) and -0.63 V (peak 2) formal potentials (green) measured using Ag/AgCl (3 M KCl) as reference electrode. These features contrast with the redox system observed for 1-aminoanthraquinone in solution which was characterized by a single reversible redox peak at a formal potential of -0.65 V at pH 7 (Figure S2).

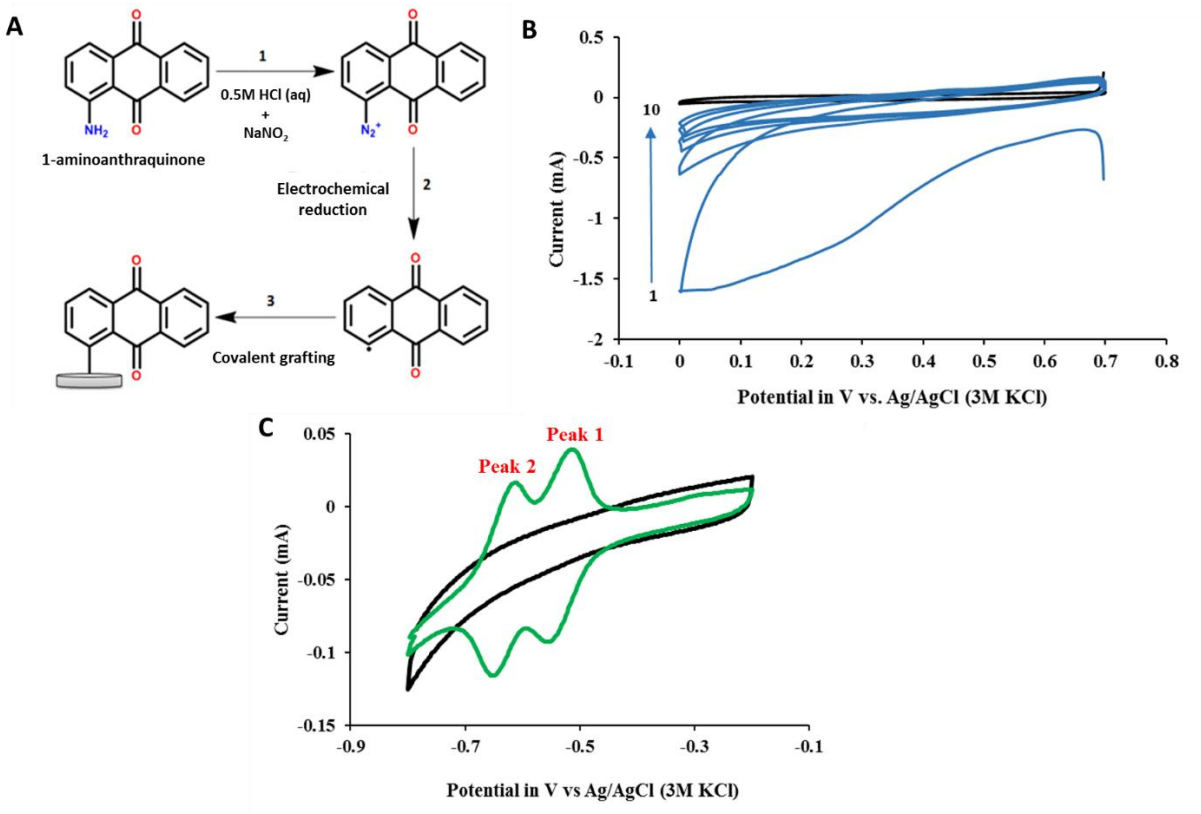


Fig. 1. 1-AAQ electrografting by in-situ cathodic reduction of the aryldiazonium salt. (A) Schematic representation of the reaction mechanism. (B) Cyclic voltammograms (10 cycles) recorded at 50 mV/s in 0.5 M acidic solution containing 1 mM 1-AAQ (black curve) with 3 mM $NaNO_2$ (blue curve). (C) Cyclic voltammetry curves of bare (black curve) and 10-AQ modified electrode after 3 min sonication (green curve) recorded at 50 mV/s in 0.1 M potassium phosphate buffer solution at pH 7.

Unlike other quinone-like moieties like catechol, which give a single redox couple after grafting or in solution [27,28] AQ is greatly affected by the pH of the electrolyte and thus the shape of the AQ redox response can be highly variable [25,29,30]. Indeed, the reduction of anthraquinone in aqueous medium is described as a multistep mechanism [31]. Although the cyclic voltammograms presented in Fig. 1C were recorded in phosphate buffer (pH 7), the previous grafting step was achieved in 0.5 M HCl and the 3 min sonication step is probably not enough to increase the local pH at the graphite electrode surface which is highly porous. Hence the slightly acidic local pH onto the electrode surface leads to the presence of two reversible redox systems in the electrochemical response of grafted AQ moieties that corresponds to an equilibrium between monoprotonated and deprotonated AQ species [29,30]. To support this hypothesis, different sonication times of 10-AQ modified electrodes in phosphate buffer were tested to see its effect on the chemical stability of the molecule and

influence on the electrochemical signal. Fig. 2 shows the changes on the CV shape of the 10-AQ grafted molecules after 3 minutes and 75 minutes of sonication. As can be seen, after 75 minutes of sonication, peak 1 (E = -0.55 V) is no longer visible while peak 2 (E = -0.63 V) remains (see also Fig. S3 for scanning electron microscope images of the electrodes before and after sonication). Furthermore, it can also be seen that the current of peak 2 has roughly doubled which is in agreement with the previous work reported elsewhere [30]. Thus, after 75 minutes of sonication in 0.1 M potassium phosphate buffer (pH 7) the remaining protons from the HCl solution are completely removed from the electrode surface. In this case, the AQ electrochemical response is a well-defined reversible redox system similar to those obtained for AQ modified electrodes under unbuffered conditions [25,30]. The surface AQ concentration (Γ) was determined by charge integration under the CV peaks: $\Gamma = Q/nFA$, where Q is the amount of charge passed, n is the number of electrons (n = 2), F is the Faraday constant and A is the electrode geometric surface area. In our experimental conditions, the 3 mm diameter electrode surface was modified with an AQ surface concentration of $2.0 \pm 0.3 \times 10^{-9}$ mol/cm^2 close to previous reported values [24,25,31].

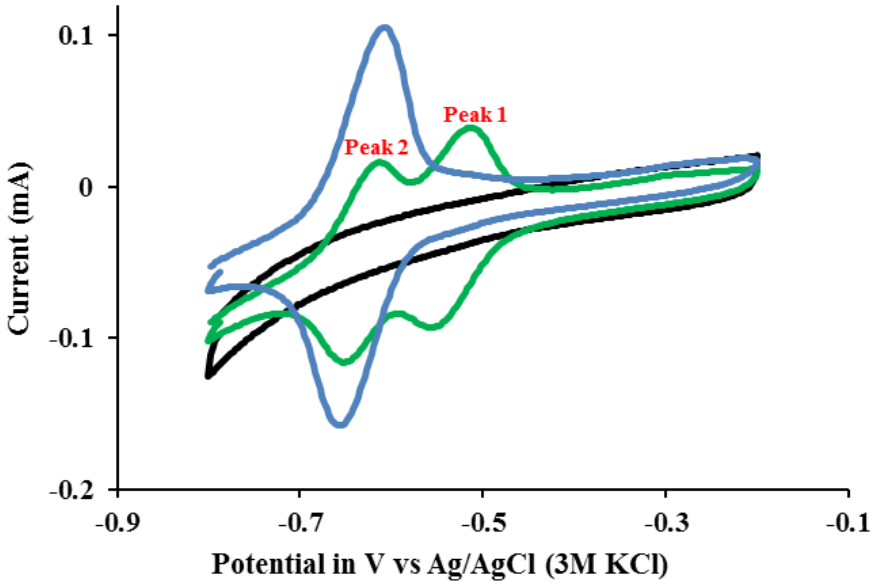


Fig. 2. Cyclic voltammetry of bare (black) and 10-AQ modified electrodes after 3 minutes (green) and 75 minutes (blue) of sonication recorded at 50 mV/s in 0.1 M potassium phosphate buffer at pH 7.

Fig. 3 shows the stability of 10-AQ modified electrode after 1 month of incubation in phosphate buffer at pH 7. During this experimental time, both reduction and oxidation peaks

became wider and slightly shifted in opposite potential directions compared with the reference electrochemical response obtained at day 1. However, the midpoint potential of the 10-AQ did not change during this time and the peak currents allowed to estimate a near quantitative stability of ca. 95% over one-month. Our results corroborate the study of Tang *et al*. [21] where a similar stability pattern was also reported. These results proved that 10-AQ was successfully grafted onto graphite electrode via strong covalent bonding exhibiting a reproducible electrochemical behavior with a high stability. Furthermore, 75 min of sonication in 0.1 M phosphate buffer pH 7 led to a univocal reversible redox system allowing the following studies to be performed under physiological conditions.

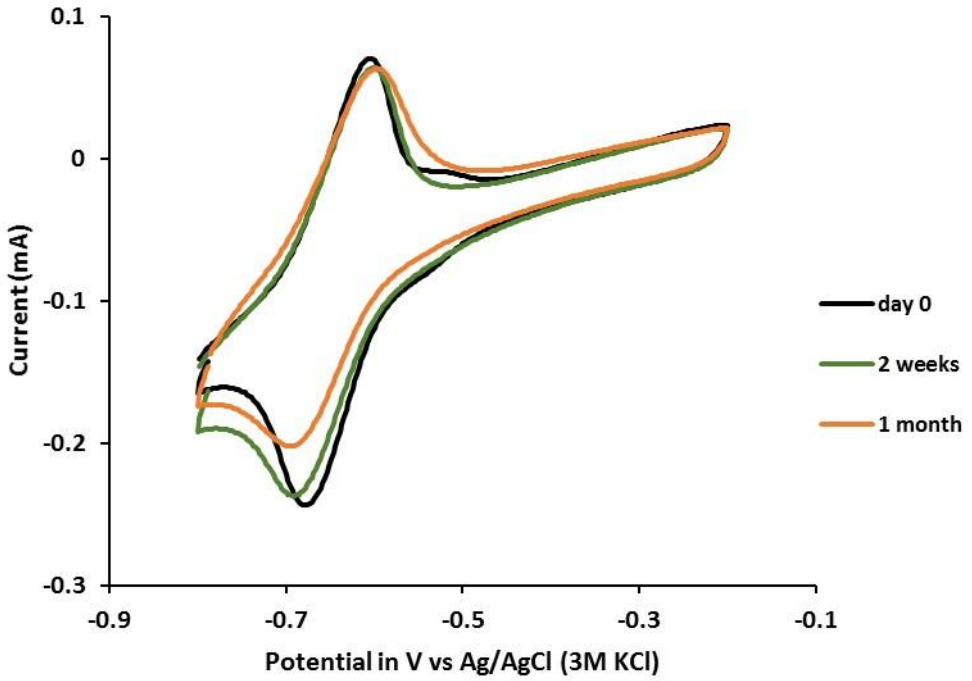


Fig. 3. Cyclic voltammetry of 10-AQ-modified electrode after 75 min sonication recorded at 50 mV/s in a 0.1 M potassium phosphate buffer aqueous solution at pH 7.

3.2 *Effect of pH on the surface of the anthraquinone-modified graphite*

The evolution of the formal potential of the anthraquinone / anthrahydroquinone redox couple with the pH of the electrolyte solution in the pH range 1-10 is shown in Fig. 4. The formal potential of electrografted 10-AQ is sensitive to pH variation with a slope of -64 mV per pH unit which is consistent with quinone-like redox systems where two electrons for two protons are exchanged [27,28,32] and with reports on other AQ-modified electrodes [33]. Thus, if the redox potential of the 10-AQ-modified electrode is compatible (i.e. different enough) with that of the biofilm and if the biofilm coverage does not conceal or destroy the pH-dependent

electroactivity of the grafted AQ, this modified electrode would then be an ideal candidate to monitor the pH of the biofilm-anode interface in MFC studies.

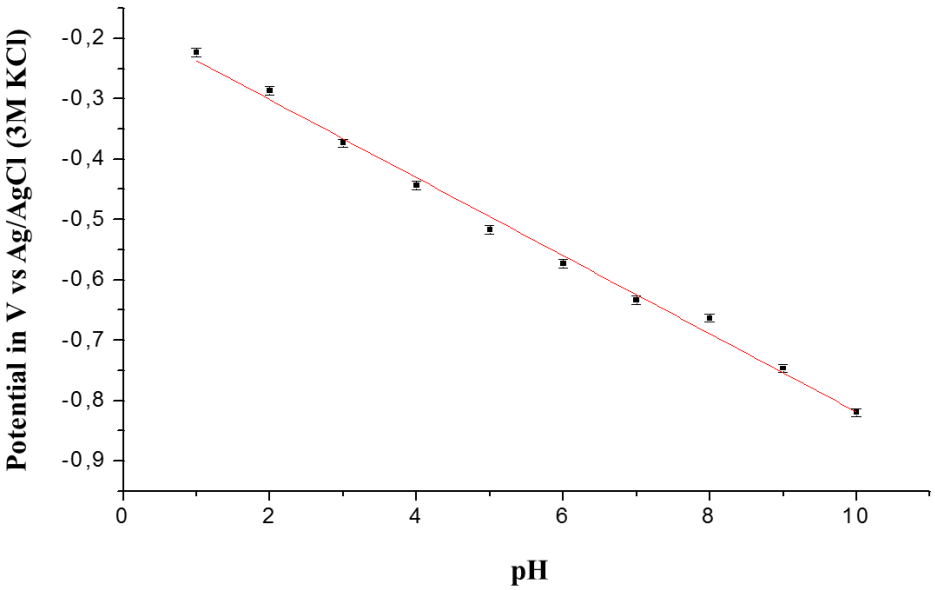


Fig. 4. Variation of the formal potential of electrografted 10-AQ as a function of the pH of the electrolyte solution obtained from three independent tests. Bars represent the standard deviation calculated from the 3 independent measurements.

3.3 *Biofilm formation onto AQ-functionalized electrodes*

Biofilm formation on the surface of bare and 10-AQ modified graphite electrode is depicted in Fig. 5. In Fig. 5A an anodic biofilm showing an asymmetric redox system with $E^{0'}$ = -0.2 V *vs.* Ag/AgCl (3 M KCl) was obtained. The microbial and electrochemical features shown by this biofilm resembles those already described for *Enterococcus spp*. This genus includes enteric and human pathogenic Gram-positive bacteria that are gaining momentum as model weak electricigen [34-36]. Considering that the bacterial inoculum used in this study is mainly municipal wastewater, the prevalence of such bacteria is likely. Moreover, the lack of bacterial redox signals at potentials more cathodic than -0.3 V, which is the case of the present biofilm, is ideal to study the putative interfacial pH changes using grafted AQ as a probe since at a physiological pH, ranging from 5 to 7, its formal potential is set between -0.5 V up to -0.65 V *vs.* Ag/AgCl (3 M KCl). Thus, the large potential separation between the electroactivity of the biofilm and the 10-AQ redox peaks is suitable to monitor pH changes upon biofilm formation on the surface of the electrode. This situation is well illustrated in Fig. 5B where the biofilm formation on the surface of 10-AQ modified electrode was monitored

for the first 3 days. On day 1, only the 10-AQ redox couple ($E^{0'}$ = -0.65 V) is observed (black CV). However, after 24 hours, a clear redox couple at $E^{0'}$ = -0.2 V was observed alongside with 10-AQ probe (Fig.5B, red CV) which suffers a decrease on the faradic current. By day 3, the 10-AQ is almost undetectable (Fig.5B, green CV). Since the main goal is to follow the interfacial pH change during biofilm formation on surface of electrodes in operating MFC, a 3-day life span for the detection of the pH redox probe is not sufficient. To overcome this situation, optimization tests were performed using different 1-AAQ deposition conditions that ranged from 20 to 80 cycles of electrografting by CV (Figure S4 A).

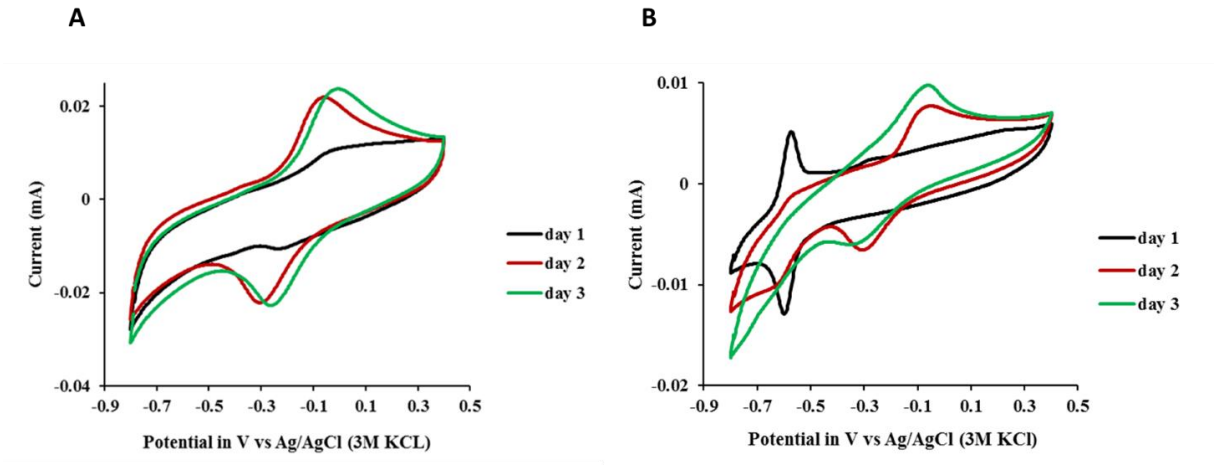


Fig. 5. Biofilm formation on bare graphite electrode (A) and 10-AQ modified electrode (B). Cyclic voltammetry recorded at 50 mV/s in anolyte of MFC at pH 7.

According to our study, 40 cycles of 1-AAQ deposition are the minimum electrografting condition required to obtain the maximum AQ faradic current on the surface of the electrode. However, this modified electrode leads to impairment of biofilm formation on the surface of the electrode (Figure S4 B). This is due to the total coverage of the electrode surface by the AQ molecules which leaves no available surface for the direct contact between the biofilm and the surface of the electrode. Notwithstanding, electrografting by 20 cycles in 1-AAQ solution (20-AQ) after 75 min sonication i.e. $6 \pm 1 \times 10^{-9}$ mol.cm^{-2}, proved to show a good compromise for electrochemical responses with those of both 20-AQ and the biofilm perfectly detectable after 21 days incubation in the anolyte, Fig. 6. With this new modified electrode (20-AQ), it was possible to follow and calculate the pH changes at the biofilm-electrode interface during bacterial growth (Table 1). Namely, the E°' of the redox probe was first calculated as the half-sum of the anodic and cathodic peak potentials of the reversible response of the grafted AQ redox probe. Then, the interfacial pH was determined using the

linear regression of the variation of the formal potentials of 10-AQ modified electrode with the pH (Fig.4).

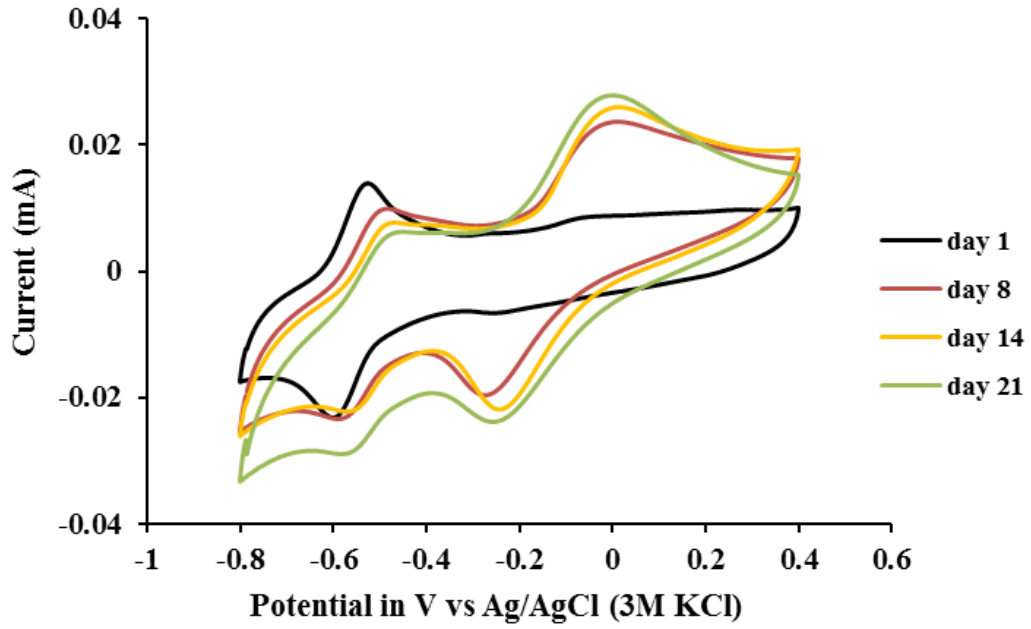


Fig. 6. Biofilm formation on 20-AQ-modified electrode. Cyclic voltammograms recorded at 50 mV/s in anolyte of MFC at pH 7.

Table 1

Evolution of the formal potential of the grafted anthraquinone on the 20-AQ-modified electrode (V *vs.* Ag/AgCl), anolyte pH and calculated biofilm interfacial pH measured over three weeks.

Time (days)	E°' 20-AQ (Volt)	Anolyte pH	Interfacial pH
0	-0.59	7.00	7.00
1	-0.56	6.70	6.40
8	-0.54	6.50	5.80
14	-0.52	6.30	5.50
21	-0.51	6.20	5.30

The change of the biofilm-electrode interfacial pH during biofilm development is monitored by the potential of the grafted anthraquinone that shifts from $E^{0'}$ = -0.56 ± 0.01 V at day 1 to -0.51 ± 0.01 V at day 21 and which corresponds to an interfacial pH change from 6.40 to 5.30 ± 0.15 respectively (Table 1). Weekly additions of 10 mM glucose led to continuous growth of the biofilm and therefore to the continuous acidification at the biofilm-electrode interface.

This is a result of the net increase of protons release in the extracellular medium during the catabolism and biocatalysis of glucose oxidation by the biofilm, Equation (1).

(1) $C_6H_{12}O_6 + 6H_2O \rightarrow 6CO_2 + 24H^+ + 24e^-$

The calculated interfacial pH revealed a continuous acidification from neutrality down to 5.30 over three weeks (Table 1) while the anolyte only acidified down to pH 6.2 over this period. Our results are in agreement with previous studies where the variation of interfacial pH in *G. sulfurreducens* biofilms were measured, showing also a 1 pH unit variation between the anolyte and the vicinity of the electrode surface (bacteria-electrode interface) [13,37]. Unlike the latter studies, here a direct modification of the surface of the electrode with a pH sensitive probe was achieved, allowing to measure the interfacial pH variation throughout the area of the electrode. Furthermore, surface modification of electrodes can also play a pivotal role on eliciting bacterial adhesion and therefore fast biofilm formation, current production and power outputs on MFC [38,39]. In this study however, the 20-AQ modified electrode has no influence on the biofilm formation and growth since it maintains the same growing pattern observed on non-modified electrodes (Fig. 5A). Moreover, the biofilm kept growing and experienced an increase in both faradic and capacitive current over 37 days, Fig. S5. This result demonstrates that the grafted pH sensor was no impairment in biofilm formation, being thus fully biocompatible.

Overall, our results demonstrate the suitability of using grafted pH sensitive molecules like AQ-based moieties as interfacial pH probes during biofilm formation on MFC electrodes. The specific pH redox probe used here however, is not applicable for biofilms with $E^{0'}$ falling between -0.4 V and -0.6 V *vs.* Ag/AgCl (3 M KCl), i.e., in the same potential window of the AQ redox response. This is the case of biofilms formed by representative Gram-negative and Gram-positive electroactive bacteria like *G. sulfurreducens* [40] and *Thermincola spp* [41,42] that display an electroactivity reported to fall between -0.4 V and -0.6 V *vs.* Ag/AgCl (3 M KCl). Notwithstanding, the AQ pH probe could be suitable to study other microbial biofilms that don't rely on low potential multiheme *c*-type cytochromes to perform the extracellular electron transfer in MFC and which electroactivity and interfacial electron transfer still remain to be unraveled. Additionally, the redox potential of the grafted pH probe may be tuned through careful selection of the substituents on different aryl amino-quinones used to generate the aryl diazonium salt.

4. Conclusions

Carbon substrates metabolism by electroactive biofilms provokes anolyte acidification and local pH changes at the electrode-biofilm interface. These local pH changes were measured using 1-aminoanthraquinone-modified electrodes as immobilized redox active pH probes which allowed to monitor a decrease of the interfacial pH from neutrality down to 5.3 over 21 days of biofilm development in neutral phosphate buffer. To our knowledge, this was the first study that showed the additional advantage of grafted quinone as a highly sensitive platform to measure pH fluctuations in a biofilm growing on the electrode surface. The biofilm studied in this work was primarily grown with glucose as the carbon source. Additionally, it presented some *Enterococcus spp*-like features, namely the asymmetric CV curve with formal potential at -0.2 V *vs.* Ag/AgCl (3 M KCl). Considering the growing interest on weak electricigens as a mean to understand the mechanisms underlying extracellular electron transfer in response to sudden changes on bacterial local environment like pH, further identification and characterization of this bacterial growing community will be interesting for the screening of wastewater microbial population, especially because enteric microorganisms are widely present in such carbon matter sources.

CRediT authorship contribution statement

Nazua L. Costa: Data curation; Formal analysis; Investigation; Supervision; Validation; Visualization; Writing - original draft, review & editing. **Germaine Olorounto**: Data curation; Investigation; Visualization. **Estelle Lebègue**: Formal analysis; Supervision; Validation; Writing - review & editing. **Frédéric Barrière**: Conceptualization; Formal analysis; Funding acquisition; Methodology; Project administration; Supervision; Writing - original draft; review & editing.

Declaration of Competing Interest

The authors declare that they have no known competing financial interests or personal relationships that could have appeared to influence the work reported in this paper.

Acknowledgements

Région Bretagne is thanked for funding a postdoc position under the Stratégie d'Attractivité Durable program 2016 (project 9621).

Appendix A. Supplementary data

Supplementary material related to this article can be found, in the online version, at doi:

References

[1] V.G. Debabov, Microbiology 77 (2008) 123–131.
https://doi.org/10.1134/S002626170802001X

[2] D.R. Lovley, Nat. Rev. Microbiol. 4 (2006) 497–508.
https://doi.org/10.1038/nrmicro1442

[3] B.E. Logan, R. Rossi, A. Ragab, P.E. Saikaly, Nat. Rev. Microbiol. 1 (2019) 307–319.
https://doi.org/10.1038/s41579-019-0173-x

[4] N.L. Costa, T.A. Clarke, L.-A. Philipp, J. Gescher, R.O. Louro, C. M. Paquete, Bioresour. Technol. 255 (2018) 308–317.
https://doi.org/10.1016/j.biortech.2018.01.133

[5] O.M.H. Richter, B. Ludwig, Biochimica et Biophysica Acta (BBA) - Bioenergetics 1787 (2009) 626–634.
https://doi.org/10.1016/j.bbabio.2009.02.020

[6] K. Rabaey, L. Angenent, U. Schröder, J. Keller (Eds.) Bioelectrochemical systems: from extracellular electrons transfer to biotechnological application. IWA Publishing, London, 2010.
https://doi.org/10.2166/9781780401621

[7] A. Bergel, BIO Web of Conferences 6 (2016) 02005.
https://doi.org/10.1051/bioconf/20160602005

[8] C.I. Torres, A.K. Marcus, B.E. Rittmann, Biotechnol. Bioeng. 100 (2008) 872–881.
https://doi.org/10.1002/bit.21821

[9] S.A. Patil, F. Harnisch, C. Koch, T. Hübschmann, I. Fetzer, A.A. Carmona-Martínez, S. Müller, U. Schröder, Bioresour. Technol. 102 (2011) 9683–9690.
https://doi.org/10.1016/j.biortech.2011.07.087

[10] J. M. Vroom, K.J. De Grauw, H.C. Gerritsen, D.J. Bradshaw, P.D. Marsh, G.K. Watson, J.J. Birmingham, C. Allison, Appl. Environ. Microbiol. 65 (1999) 3502–3511.
https://doi.org/10.1128/AEM.65.8.3502-3511.1999

[11] R.C. Hunter, T.J. Beveridge, Appl. Environ. Microbiol. 71 (2005) 2501–2510.
https://doi.org/10.1128/AEM.71.5.2501-2510.2005

[12] S. Schlafer, J.E. Garcia, M. Greve, M.K. Raarup, B. Nyvad, I. Dige, Appl. Environ. Microbiol. 81 (2015) 1267–1273.
https://doi.org/10.1128/AEM.02831-14

[13] J.T. Babauta, H.D. Nguyen, T.D. Harrington, R. Renslow, H. Beyenal, Biotechnol. Bioeng. 109 (2012) 2651–2662.
https://doi.org/10.1002/bit.24538

[14] F.M. Boldt, J. Heinze, M. Diez, J. Petersen, M. Börsch, Anal. Chem. 76 (2004) 3473–3481.
https://doi.org/10.1021/ac049635x

[15] L. Poltorak, M. Hébrant, M. Afsharian, M. Etienne, G. Herzog, A. Walcarius, Electrochim. Acta. 188 (2016) 71–77.
https://doi.org/10.1016/j.electacta.2015.11.107

[16] M. Michalak, M. Kurel, J. Jedraszko, D. Toczydlowska, G. Wittstock, M. Opallo, W. Nogala, Anal. Chem. 87 (2015) 11641–11645.
https://doi.org/10.1021/acs.analchem.5b03482

[17] S. Fulaz, S. Vitale, L. Quinn, E. Casey, Trends Microbiol. 27 (2019) 915–926.
https://doi.org/10.1016/j.tim.2019.07.004

[18] S. Fulaz, D. Hiebner, C.H.N. Barros, H. Devlin, S. Vitale, L. Quinn, E. Casey, ACS Appl. Mater. Interfaces 11 (2019) 32679–32688.
https://doi.org/10.1021/acsami.9b09978

[19] V.G.H. Lafitte, W. Wang, A.S. Yashina, N.S. Lawrence, Electrochem. Commun. 10 (2008) 1831–1834.
https://doi.org/10.1016/j.elecom.2008.09.031

[20] A.S. Kumar, P. Swetha, Colloids and Surfaces A: Physicochem. Eng. Aspects 384 (2011) 597–604.
https://doi.org/10.1016/j.colsurfa.2011.05.010

[21] X. Tang, H. Li, Z. Du, H. Y. Ng, Bioresour. Technol. 164 (2014) 184–188.
https://doi.org/10.1016/j.biortech.2014.05.010

[22] H. Smida, E. Lebègue, M. Cortes, J.-F. Bergamini, F. Barrière, C. Lagrost, Bioelectrochemistry 125 (2019) 70.
https://doi.org/10.1016/j.bioelechem.2018.07.012

[23] H. Smida, E. Lebègue, J.-F. Bergamini, F. Barrière, C. Lagrost, Bioelectrochemistry, 120 (2018) 157–165.
https://doi.org/10.1016/j.bioelechem.2017.12.006

[24] M. Kullapere, J.M. Seinberg, U. Mäeorg, G. Maia, D.J. Schiffrin, K. Tammeveski, Electrochim. Acta 54 (2009) 1961–1969.
https://doi.org/10.1016/j.electacta.2008.08.054

[25] M. Weissmann, O. Crosnier, T. Brousse, D. Bélanger, Electrochim. Acta 82 (2012) 250–256.
https://doi.org/10.1016/j.electacta.2012.05.130

[26] S. Baranton, D. Bélanger, J. Phys. Chem. B 109 (2005) 24401–24410.
https://doi.org/10.1021/jp054513+

[27] E. Lebègue, R.O. Louro, F. Barrière, ACS Omega 3 (2018) 9035–9042.
https://doi.org/10.1021/acsomega.8b01425

[28] E. Lebègue, N.L. Costa, B.M. Fonseca, R.O. Louro, F. Barrière, J. Electroanal. Chem. 847 (2019) 113232.
https://doi.org/10.1016/j.jelechem.2019.113232

[29] G. Jürmann, D.J. Schiffrin, K. Tammeveski, Electrochim. Acta 53 (2007) 390–399.
https://doi.org/10.1016/j.electacta.2007.03.053

[30] C. Batchelor-Mcauley, B.R. Kozub, D. Menshykau, R.G. Compton, J. Phys. Chem. C 115 (2011) 714–718.
https://doi.org/10.1021/jp1096585

[31] S. Baranton, D. Bélanger, Electrochim. Acta 53 (2008) 6961–6967.
https://doi.org/10.1016/j.electacta.2008.02.105

[32] Q. Li, C. Batchelor-McAuley, N.S. Lawrence, R.S. Hartshorne, R.G. Compton, Chem. Commun. 47 (2011) 11426–11428.
https://doi.org/10.1039/C1CC14191K

[33] L. Devlin, M. Jamal, K. M. Razeeb, Anal. Methods 5 (2013) 880–884.
https://doi.org/10.1039/C2AY26264A

[34] L.E. Doyle, E. Marsili, Bioresour. Technol. 258 (2018) 354–364.
https://doi.org/10.1016/j.biortech.2018.02.073

[35] G.T. Kim, M.S. Hyun, I.S. Chang, H.J. Kim, H.S. Park, B.H. Kim, S.D. Kim, J.W.T. Wimpenny, A.J. Weightman, J. Appl. Microbiol. 99 (2005) 978–987.
https://doi.org/10.1111/j.1365-2672.2004.02514.x

[36] G. Pankratova, D. Leech, L. Gorton, L. Hederstedt, Biochemistry 57 (2018) 4597–4603.
https://doi.org/10.1021/acs.biochem.8b00600

[37] A.E. Franks, K.P. Nevin, H. Jia, M. Izallalen, T.L. Woodard, D.R. Lovley, Energy Environ. Sci. 2 (2009) 113–119.
https://doi.org/10.1039/B816445B

[38] M. Picot, L. Lapinsonnière, M. Rothballer, F. Barrière, Biosens. Bioelectron. 28 (2011) 181–188.
https://doi.org/10.1016/j.bios.2011.07.017

[39] L. Lapinsonnière, M. Picot, C. Poriel, F. Barrière, Electroanalysis 25 (2013) 601–605.
https://doi.org/10.1002/elan.201200351

[40] H. Richter, K.P. Nevin, H. Jia, D.A. Lowy, D.R. Lovley, L.M. Tender, Energy Environ. Sci. 2 (2009) 506–516.
https://doi.org/10.1039/B816647A

[41] B.G. Lusk, I. Peraza, G. Albal, A.K. Marcus, S.C. Popat, C.I. Torres, J. Am. Chem. Soc. 140 (2018) 5527–5534.
https://doi.org/10.1021/jacs.8b01734

[42] N.L. Costa, B. Hermann, V. Fourmond, M.M. Faustino, M. Teixeira, O. Einsle, C.M. Paquete, R.O. Louro, mBio (2019).
https://doi.org/10.1128/mBio.01210-19